How to cite: *Angew. Chem. Int. Ed.* **2021**, *60*, 21543 – 21549
International Edition: doi.org/10.1002/anie.202108698
German Edition: doi.org/10.1002/ange.202108698

Hydrogels Hot Paper

Dual-Responsive Material Based on Catechol-Modified Self-Immolative Poly(Disulfide) Backbones

Asger Holm Agergaard, Andreas Sommerfeldt, Steen Uttrup Pedersen, Henrik Birkedal, and Kim Daasbjerg**

Abstract: *Functional materials engineered to degrade upon triggering are in high demand due their potentially lower impact on the environment as well as their use in sensing and in medical applications. Here, stimuli-responsive polymers are prepared by decorating a self-immolative poly(dithiothreitol) backbone with pendant catechol units. The highly functional polymer is fashioned into stimuli-responsive gels, formed through pH-dependent catecholato–metal ion cross-links. The gels degrade in response to specific environmental changes, either by addressing the pH responsive, non-covalent, catecholato–metal complexes, or by addition of a thiol. The latter stimulus triggers end-to-end depolymerization of the entire self-immolative backbone through end-cap replacement via thiol–disufide exchanges. Gel degradation is visualized by release of a dye from the supramolecular gel as it itself is converted into smaller molecules.*

Introduction

Multi-responsive gels are an attractive class of materials with applications within areas such as delivery of therapeutics,[1] actuation,[2] and sensing.[3] The ability to engineer a material to show a specific response when exposed to certain conditions such as the presence of a specific molecule or changes in the local environment eliminates the need for human intervention, as the system responds autonomously, with a pre-programmed response. Such materials can consist of two fundamental components, a polymeric backbone structure and cross-links responsible for gelation. For delivery of small molecules, a vanishing gel is attractive as it delivers not only cargo, but also breaks down to small molecules at the destination of the cargo. This raises demand for a degradable polymer backbone, capable of forming a gel.

Recently, highly functional materials were reported in which both the polymer backbone and the cross-links possessed responsive chemistries. Zhang et al. utilized thermal ring opening polymerization of thioctic acid and subsequent carboxylate-Fe^{3+} cross-linking to generate a network polymer possessing two levels of self-healing. Rapid exchange in carboxylate-Fe^{3+} cross-links was responsible for fast formation of weak bonds in broken interfaces, and a slower disulfide exchange between backbones generated new covalent bonds at interfaces.[4]

Polyamines functionalized by polyphenols such as L-3,4-dihydroxyphenylalanine formed doubly pH-responsive hydrogels based on the acid/base chemistry of the amines and the pH-dependent metal coordination of the polyphenols.[5,6] Lu et al. reported a multi-responsive gel capable of actuation by virtue of a polyelectrolyte backbone, while also possessing the ability to be photocleaved and photocross-linked through pendant coumarin groups.[7] Chen et al. presented a multi-responsive system containing benzoxaborole ester cross-links, responsive towards pH, ATP, fructose, and H_2O_2.[8]

While the above examples contain high levels of responsivity, they all leave the intact polymer backbones after triggering responses; full deconstruction of the polymer system would in many cases be advantageous. In literature, numerous examples of polymeric systems with such a property are reported. For example, disulfide-linked cyclodextrins have been shown to exhibit responsivity toward glutathione, resulting in cleavage of polymer cross-links.[9] Chain shattering polymers that respond to either UV or thiols and released drugs/monomeric units upon exposure to triggering conditions have been reported.[10,11] Zhang et al. further reported a poly(thioctic acid) material that could enter in a recycling loop complete with polymer degradation, monomer recycling, and repolymerization.[12] Recently, self-immolative polymers (SIPs) have emerged as a unique class of stimuli-responsive polymers with the attractive trait of controlled end-to-end depolymerization upon demand.[13] Reported examples include poly(benzyl carbonates) used in sensors,[14] poly(benzyl carbamates) in point-of-care devices,[15] poly(benzyl ethers) utilized for reversible adhesion,[16] in plastics recycling,[17] and in antibacterials,[18] poly(phthalaldehydes) in smart composites,[19] polyglyoxylates exploited in degradable packaging,[20] and poly(dithiothreithol) as vanishing plastic that depolymerizes into water-soluble small molecules.[21]

[*] A. H. Agergaard, Dr. A. Sommerfeldt, Prof. S. U. Pedersen, Prof. H. Birkedal, Prof. K. Daasbjerg
Department of Chemistry, Aarhus University
Langelandsgade 140, 8000 Aarhus (Denmark)
and
Interdisciplinary Nanoscience Center (iNANO)
Aarhus University
Gustav Wieds Vej 14, 8000 Aarhus (Denmark)
E-mail: hbirkedal@chem.au.dk
kdaa@chem.au.dk

Supporting information and the ORCID identification number(s) for the author(s) of this article can be found under: https://doi.org/10.1002/anie.202108698.

© 2021 The Authors. Angewandte Chemie International Edition published by Wiley-VCH GmbH. This is an open access article under the terms of the Creative Commons Attribution Non-Commercial NoDerivs License, which permits use and distribution in any medium, provided the original work is properly cited, the use is non-commercial and no modifications or adaptations are made.

In terms of responsive cross-links, dynamic covalent bonds such as boronate esters,[22] imines,[23] and Diels–Alder adducts[24] have been explored, contributing to desirable material properties such as self-healing.[25] Non-covalent cross-links, such as catecholato–metal complexes, or chelates of carboxylates and metal ions similarly result in formation of self-healing gels.[4,26,27] Similar properties are also obtained through cyclodextrin host–guest interactions.[28]

Herein, our aim is to synthesize fully degradable and dual-responsive gels addressing both the polymer backbone and cross-linking chemistry. As for the choice of responsive backbone, we chose a SIP, given its inherent ability to be depolymerized into monomeric species in response to specific stimuli. SIP backbones are a promising class of fully degradable polymers, enabling reuse of the product at end-of-life. Recently, we expanded the SIP family with a new member, namely a self-immolative disulfide backbone, poly-(dithiothreitol) (pDTT), end-capped with thiopyridine-disulfide bonds (see structure in Scheme 1 a).[21] An attractive trait of pDTT is the ease by which it is prepared on gram scale through simple solid-state synthesis with no need of rigorously dry and inert conditions. In addition, the backbone of pDTT has hydroxy moieties, which are apt for further functionalization, making pDTT a strong candidate for a degradable scaffold in highly functional and responsive polymer systems. A third prominent feature is its rapid depolymerization in response to external stimuli. Specifically, adding dithiothreitol (DTT) results in uncapping (i.e. initiation of depolymerization) through thiol–disulfide exchange with the activated thiopyridine disulfide bonds of the end-cap moieties (see Scheme 1 b).

As for the choice of cross-linking chemistry, we find the catechol system particularly appealing. Catechol excels with its inherently versatile chemistry involving interaction through either hydrogen bonding, π–π stacking, or cross-linking through metal ion chelation.[29,30] Both catecholato–boronate[31] and catecholato–metal complexes[27,29,32] are highly responsive, and have been utilized as dynamic cross-links in functional materials. The catecholato–metal complexation with trivalent metal ions is dependent on the redox state[33] of catechol, and solution pH. Agergaard et al. utilized both properties to synthesize detachable polymer brushes, tethered to surfaces through catecholato–metal compexes.[34] Mono-catecholato–metal species are predominant at low pH, and tris-catecholato–metal complexes are abundant in alkaline environments. When catechol is attached to a polymer backbone, complexation with metal ions results in cross-links to give a pH-responsive gel. The gels have desirable properties such as self-healing, owing to the dynamic bond exchange nature of the catecholato–metal bond.[35] The physical properties of the catecholato–metal complex, for example, color and rupture force, depend on the metal ion used and its exact d-electron structure.[6,36]

Specifically, we synthesize a dual-responsive polymer and gel, denoted pDTT-Cat, where the versatile and pH-responsive metal ion cross-linking chemistry of catechol is merged with the SIP backbone of pDTT that provides on-demand degradation through self-immolative depolymerization. We demonstrate how depolymerization can result in release of rhodamine 6G dye from gels, due to material degradation to small molecules. Concurrently, gel liquefaction can be achieved when exposing the material to low pH, where the catecholato–metal cross-links are broken, resulting in disintegration of the gel, and dye release. Thus, the two mechanisms of degradation are promoted under different conditions, either at high pH in a base-catalyzed, thiol-induced depolymerization, or at low pH through the transition from tris- to mono-catecholato–metal ion complexes, effectively reversing cross-linking.

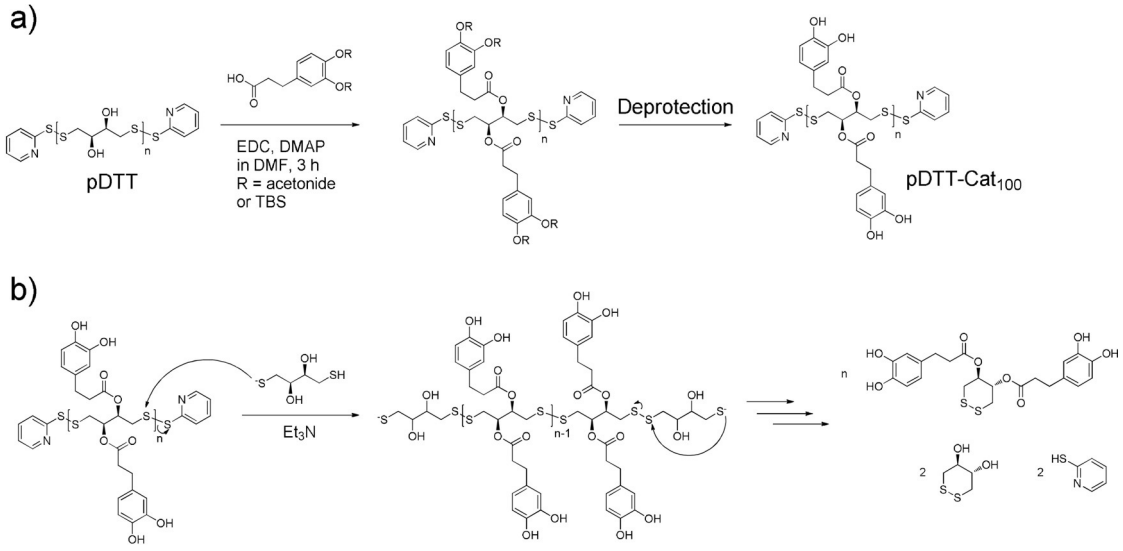

Scheme 1. a) Functionalization of pDTT using EDC coupling of protected dihydrocaffeic acid, followed by deprotection to reveal the catecholic moiety. b) Thiol-induced/base-catalyzed depolymerization of catechol-modified poly(dithiothreitol) to produce catechol-modified cDTT via cyclization reactions upon end-cap removal.

 © 2021 The Authors. Angewandte Chemie International Edition published by Wiley-VCH GmbH

Results and Discussion

Scheme 1a outlines the protocol for synthesizing catechol-modified pDTT, pDTT-Cat$_x$, where the subscript designates the catechol content which could be adjusted from 0 to 100%. First, pDTT was produced using the previously described solid-state synthesis, applying mechanical mixing (i.e. a speedmixer for 3 min) to a mixture of monomeric DTT and a thiol–disufide activating reagent, 2,2′-dithiodipyridine.[21]

Next, the carboxylic acid group on protected dihydrocaffeic acid (DHCA) was esterified with the alcohol groups on the pDTT backbone through a Steglich esterification. Conversion of backbone hydroxy groups was found to be quantitative when using 4-dimethylaminopyridine (DMAP) as esterification catalyst and 1-ethyl-3-(3-dimethylaminopropyl)carbodiimide hydrochloride (EDC·HCl) as coupling agent. Protection of catecholic hydroxy groups was essential for achieving clean reactions in fair yield. Either acetonide (Ace) or *tert*-butyldimethylsilyl (TBS) protection groups were used (Figures S1 and S2), abbreviated TBS-DHCA and Ace-DHCA, respectively. Polymers obtained from this coupling are denoted pDTT-TBS-DHCA$_x$ and pDTT-Ace-DHCA$_x$, respectively.

Specifically, we obtained pDTT-Cat$_{100}$ via the acetonide route and pDTT-Cat$_{20}$ via the silyl ether route. We note that the yield of the acetonide synthesis of pDDT-Cat$_{100}$ is low (9%), but we include pDTT-Cat$_{100}$ here for the sake of obtaining a clearer understanding of the polymer analysis. Figures S3, S4, and S5 show the ^{1}H NMR spectra of pDTT, pDTT-Ace-DHCA$_{100}$, and pDTT-Cat$_{100}$, respectively. For complete polymer composition analysis of pDTT, pDTT-Ace-DHCA$_{100}$, pDTT-Cat$_{100}$, pDTT-Ace-DHCA$_{20}$, pDTT-TBS-DHCA$_{20}$, and pDTT-Cat$_{20}$, please refer to Supporting Information (Figures S3–S8).

Figure 1a shows Size Exclusion Chromatography Multiple Angle Laser Light Scattering (SEC–MALS) traces of pDTT after successive catechol functionalization. Upon modification of pDTT with protected DHCA, the SEC trace shifts to shorter elution times as expected for larger molecules. The higher the esterification density becomes, the more unimodal the SEC trace appears, suggesting that conversion of hydroxy groups to ester functions diminishes molecular interactions in terms of hydrogen bonding. Upon protection group removal, elution volume decreases further, which we attribute to existence of strong intermolecular interactions between different polymer chains through now-revealed catechol units.[37] Such interactions include bidentate hydrogen bonding and π–π stacking. In the case of pDTT-Cat$_{20}$, we were able to substantiate such concentration-dependent interchain interactions between catechol units by comparing SEC traces of pDTT-Cat$_{20}$ and pDTT-TBS-DHCA$_{20}$ at increasing concentrations. While elution times of pDTT-Cat$_{20}$ increased at higher concentrations (Figure S9), there was no such effect for pDTT-TBS-DHCA$_{20}$ (Figure S10). Figure S11 shows the SEC traces for pDTT, pDTT-Ace-DHCA$_{20}$, and pDTT-Cat$_{20}$, and Table S1 compiles M_n, M_w, and DP parameters for all studied polymers, extracted from SEC data (see Figures S9–S13 for further discussion).

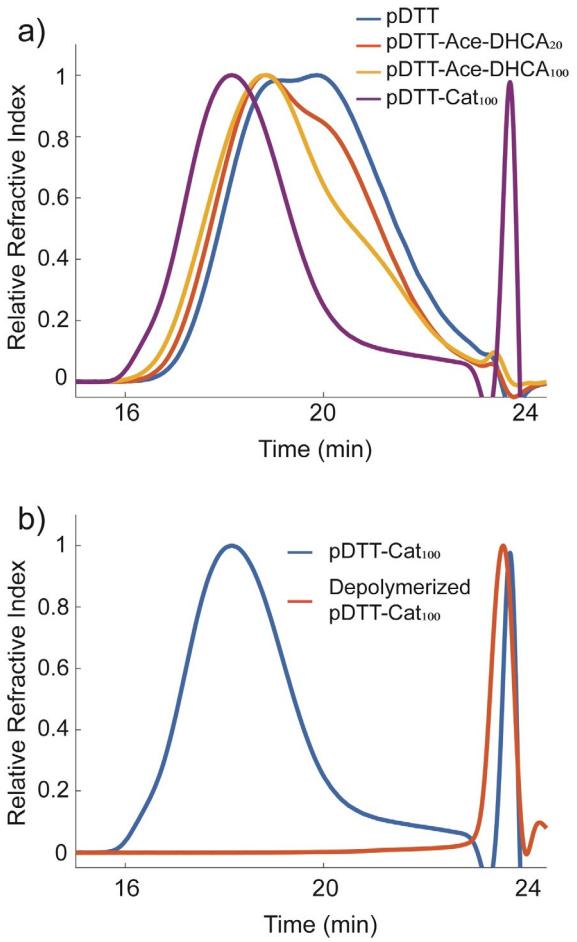

Figure 1. a) SEC traces of unmodified pDTT (blue), pDTT-Ace-DHCA$_{20}$ (orange), pDTT-Ace-DHCA$_{100}$ (yellow), and pDTT-Cat$_{100}$ (purple) in 0.01 M LiBr/DMF. The small-molecule peak at ca. 24 min is ascribed to solvent impurity as confirmed by ^{1}H NMR (Figure S5). b) SEC trace of pDTT-Cat$_{100}$ (blue) and pDTT-Cat$_{100}$ after addition of 1 equiv DTT and 0.5 equiv Et$_3$N w.r.t. end-caps (orange) in 0.01 M LiBr/DMF. All sample concentrations were 4 mg mL^{-1}.

Degradability of Modified pDTT

Scheme 1b shows the proposed reaction transforming pDTT-Cat to small molecules on the basis of the already known depolymerization pathway of pDTT itself.[21] This ability to degrade on demand through a self-immolative process by exposure to specific stimuli is a key property of the novel multifunctional polymer. Specifically, by cleaving off the end-caps with a stoichiometric amount of DTT (i.e. 1 equiv per end-cap), the unstable polymer backbone initiates depolymerization through a cascade of cyclizations. This involves a sequence of base-catalyzed ring-closing thiol–disulfide exchanges, to give the thermodynamically stable and esterified form of 1,2-dithiane-4,5-diol cyclic product (cDTT), which is the oxidized and ring-closed form of DTT. To promote faster thiol–disulfide exchange kinetics, a catalytic amount of base (0.5 equiv Et$_3$N per end-cap) was added to increase the concentration of the more reactive thiolate species.

 © 2021 The Authors. Angewandte Chemie International Edition published by Wiley-VCH GmbH

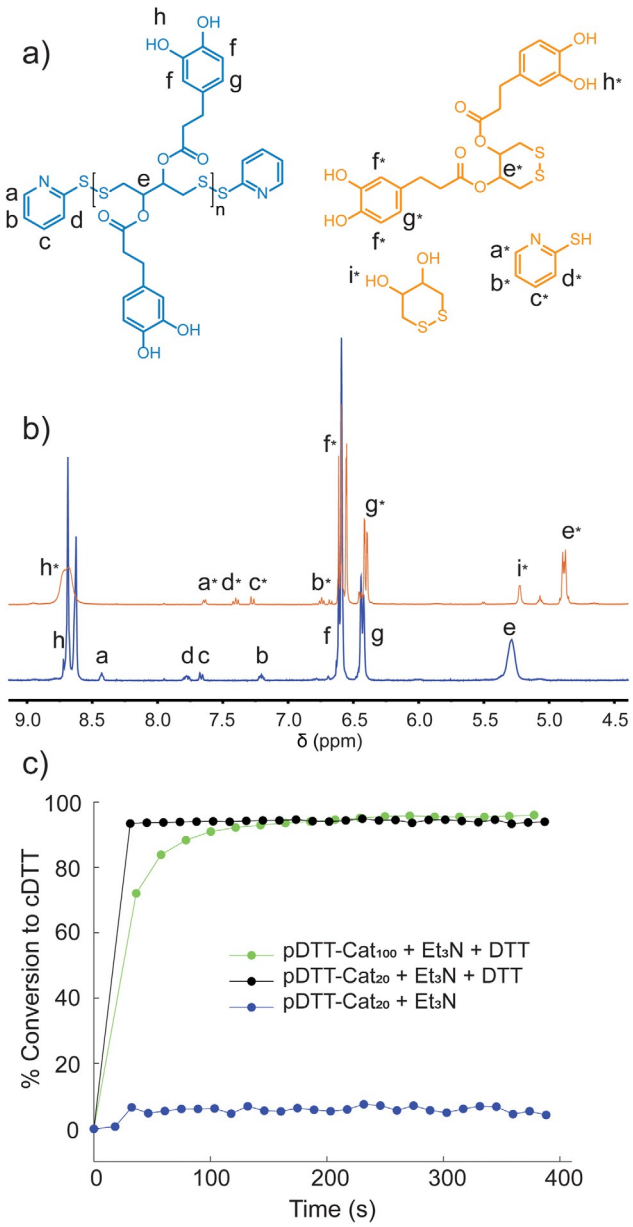

Figure 2. a) Chemical structure of depolymerization products from pDTT-Cat_{100}. b) ^{1}H NMR of pDTT-Cat_{100} (blue) and pDTT-Cat_{100} depolymerized in presence of 1 equiv DTT and 0.5 equiv Et_3N with respect to polymer end-caps (orange) in DMSO-d_6. c) Conversion of polymers, pDTT-Cat_{100} (green), and pDTT-Cat_{20} (black) to cyclic monomer in response to adding 1 equiv DTT and 0.5 equiv Et_3N, along with the response of adding only 0.5 equiv Et_3N to pDTT-Cat_{20} (blue), measured by ^{1}H NMR spectroscopy (lines to guide the eye). In all measurements the polymer concentration was 1.6 mM.

Figure 2 a,b shows how the transformation of pDTT-Cat_{100} from polymer to small molecules is reflected in ^{1}H NMR. Upon uncapping, the peaks assigned to end-caps all shift downfield when pyridine-2-thiol is released in accordance with our previous report.[21] The progress of depolymerization is indicated by decrease of the peak at 5.28 ppm, associated with C**H**-O(CO)- in pDTT-Cat_{100}, while a new peak at 4.89 ppm is ascribed to the same proton in the cyclic monomer, cDTT-$(Cat)_2$ (Figure S14). A peak at 5.23 ppm, assigned to CH-O**H** in cDTT, originates from the DTT added to remove end-caps (Figures S14–S16 display full spectra and assignments of depolymerization products from pDTT-Cat_{100}).

Figure 1 b shows corresponding SEC data where a change occurs from large hydrodynamic radius with elution times of 16–21 min to small molecule fragments with elution time of 24 min upon uncapping and depolymerization. This signifies that the self-immolative property of the pDTT backbone is preserved after modification with catechol. Similarly, degradation of pDTT-Cat_{20} was characterized by ^{1}H NMR (Figures S17 and S18) and SEC (Figure S19). Evident from the SEC data, the products obtained from degradation of pDTT-Cat_{20} result in several peaks, corresponding to cDTT (27 min) and cDTT-$(Cat)_1$ with one catechol unit (25 min) along with a peak ascribed to an unknown solvent impurity (24 min). Figure S19 also shows the SEC trace of degradation products from pDTT-Cat_{100}, which results in a single peak assigned to cDTT-$(Cat)_2$ (23 min).

To investigate the possibility of inter-chain disulfide exchange and macrocycle formation, we studied degradation of unmodified pDTT in a more concentrated solution (40 mM vs. 1.6 mM in standard degradation experiments) to promote possible inter-chain reactions. By adding 0.25 equiv DTT w.r.t. end-caps, only every other chain is expected to depolymerize if no inter-chain depolymerization occurs. SEC traces showed formation of only small molecules (Figure S20) which indicates that some inter-chain depolymerization may take place, however without resulting in larger macrocyclic structures. Most likely, this observation can be attributed to a situation where the smallest (and thus fastest diffusing) depolymerizing thiolate ends attack new chains, thus inducing depolymerization.

Figure 2 c displays kinetic traces of the degradation processes of pDTT-Cat_{100} and pDTT-Cat_{20}, respectively. Depolymerization was taken as the percentage conversion to cyclic monomer species against time, determined by ^{1}H NMR analysis (Figures S16 and S17). As seen, both polymers exhibit complete degradation in DMSO-d_6 within a few minutes of adding DTT and Et_3N. In fact, degradation of pDTT-Cat_{20} occurs essentially within the 30 s needed to record the first NMR spectrum. Depolymerization of pDTT-Cat_{100} is slower than that of DTT-Cat_{20}, which we ascribe to the higher content of bulky catechol substituents, slowing the ring-closing reaction. In addition to steric effects, the relatively low pK_a of the catechol hydroxy groups may reduce the efficiency of the base catalysis.[38] Nevertheless, the response of pDTT-Cat_{100} to chemical stimuli (i.e. DTT/Et_3N) is rapid, with full depolymerization accomplished within 3 min. Evident from Figure 2 c, adding Et_3N alone does not induce depolymerization or end-cap removal on the timescale of these degradation experiments.

The facile depolymerization of pDTT-Cat_x is crucial for the intended degradation of gels cross-linked by catecholato–metal ion complexes, as steric constraints imposed by the cross-links is expected to slow down the disulfide cyclization reaction further, thus reducing depolymerization rate. In this study, we did not attempt to isolate and recycle the monomeric species from the depolymerization, but we have

 © 2021 The Authors. Angewandte Chemie International Edition published by Wiley-VCH GmbH

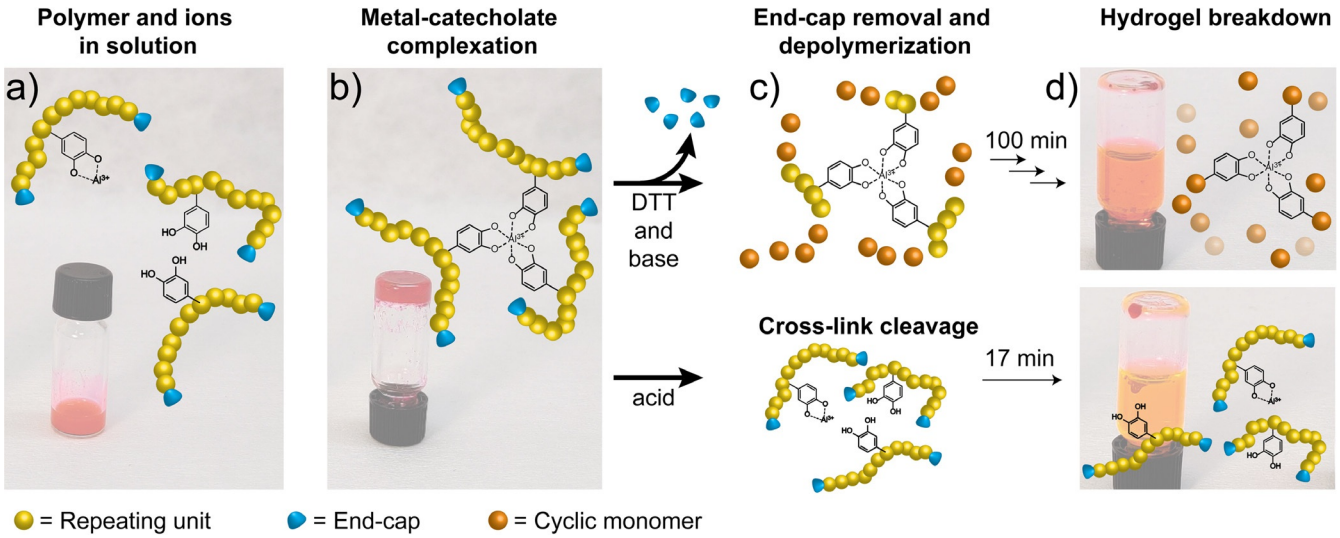

Figure 3. a) pDTT-Cat_{20}, Al^{3+}, and rhodamine 6G in solution and b) after inducing hydrogel formation by addition of NaOH to raise pH (>10). c) Mechanism of gel breakdown, induced either by depolymerization through decapping by addition of 10 equiv DTT and 5 equiv Et_3N w.r.t. end caps (top), or by cleavage of Al^{3+}–catecholato cross-links at low pH, by addition of 1 M HCl in MeOH (bottom). d) Resulting liquefaction of the hydrogel and concomitant release of rhodamine 6G into solution after 100 min (depolymerization) and 17 min (catecholato–metal cross-link cleavage).

previously reported the recovery and repolymerization of cDTT obtained from depolymerization of pristine pDTT.[21]

Hydrogel Formation

Figure 3 establishes a key feature of polymers decorated with catechol pendant groups, which is the ability to form gel networks through formation of catecholato–metal cross-links. In this study, hydrogels were formed and loaded with dye (for visualization) by first dissolving pDTT-Cat_{20} in a solution of rhodamine 6G in MeOH, and adding a solution of Al^{3+} ions to produce the mono-catecholato–Al^{3+} species (Figure 3a). To induce cross-linking, pH was raised by addition of aqueous NaOH, resulting in immediate hydrogelation with the dye trapped in the gel (Figure 3b). Formation of catecholato–Al^{3+} species is pH-dependent, forming predominantly mono-, bis-, and tris-complexes at acidic, intermediate, and alkaline pH respectively.[6,39]

Triggered Hydrogel Degradation

Figure 3c,d demonstrates the stimuli-triggered response of gels made from pDTT-Cat_{20}, rhodamine 6G dye, and Al^{3+}, after addition of DTT/Et_3N in MeOH or 1 M HCl in MeOH, either of which results in complete gel liquefaction. Importantly, this confirms successful introduction of dual stimuli-responsiveness into the gels through the self-immolative backbone and the catecholato–metal cross-links. Notably, the time scale for these two types of gel liquefaction is different, in that cleavage of cross-links is complete within 17 min, while depolymerization takes at least 100 min (Figure S21 and Movie S1 in Supporting Information). As such, the two functionalities represent two orthogonal pathways to hydrogel degradation, working in different time regimes. While catecholato–metal cross-links addressed by lowering pH respond relatively fast, the depolymerization triggered by addition of DTT is, at least, five times slower. We note that the response time is minutes to a few hours, and thus the translation of a molecular trigger to a macroscopic response can be considered as rapid. Compared to previously reported degradable gels based on breaking disulfides, this depolymerization reaction results in a swift degradation, with the option for even faster responsivity through the acid-labile cross-links.[9,10,40]

Figure 4 shows the absorbance in UV/Vis caused by release of rhodamine 6G from the gels as function of time using the two stimuli (see Figures S22–S24 for raw UV

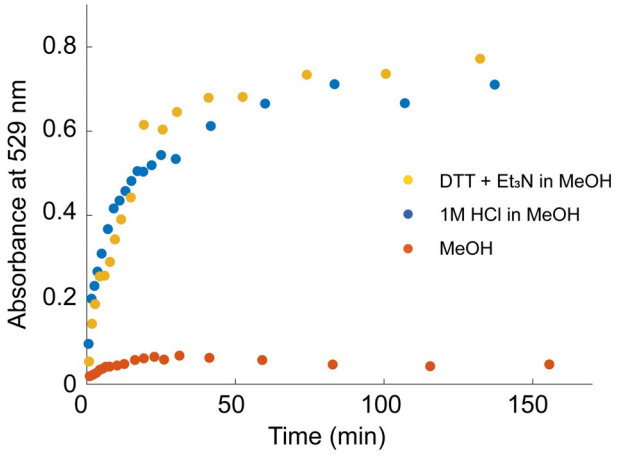

Figure 4. Dye release from pDTT-Cat_{20} gels in different environments measured as absorbance at 529 nm; 1 M HCl in MeOH (blue), 10 equiv DTT and 5 equiv Et_3N (with respect to end-caps) in MeOH (yellow), MeOH without stimuli (orange). Dashed lines to guide the eye.

 © 2021 The Authors. Angewandte Chemie International Edition published by Wiley-VCH GmbH

spectra). The important revelation of this experiment is that the macroscopic response (increase in absorbance from the released dye) to a molecular signal is significant, no matter which of the stimuli-responsive moieties is addressed. Thus, the pDTT-Cat_{20} gel can, potentially, work as drug carrier with the self-immolative backbone or the metal–catecholato cross-links as release functions. Note that the release is, by and large, completed within one hour, independent of the selected stimuli-responsive moiety. This similarity of the results is not particularly surprising, as the release of a given molecule from a hydrogel breaking up consists of additional steps than the responsiveness actions themselves, for example, diffusion of small molecules and changes in polymer chain conformation. Thus, different regimes of mass transport would need to be considered if a thorough evaluation of the kinetics was the goal. In addition, the experimental conditions were not exactly the same in the experiments presented in Figures 3 and 4. While the gels depicted in Figure 3 were left unperturbed for gel degradation until pictures were captured, the corresponding solutions above the gels for the small molecule release measurements (Figure 4) were homogenized immediately prior to withdrawing each sample (see Supporting Information). Nonetheless, the experiments work nicely as proof-of-concept illustrations of the dual-responsiveness of the gels.

Finally, regeneration of gels from the acidic solution resulting from cleaving catecholato–Al^{3+} cross-links was attempted by raising pH once again. However, addition of aqueous NaOH resulted in formation of smaller, individual gel particles rather than a single, large gel. We ascribe this to the significant dilution of the polymer chains when attempting direct gel reforming (starting concentration of $\approx 110\ mg\,mL^{-1}$ compared to a final concentration of $\approx 25\ mg\,mL^{-1}$). Formation of smaller gel particles may find use in for example, drug formulation within the gels.

Conclusion

We have presented a responsive polymer consisting of a self-immolative backbone decorated with catechol units. Through catecholato–Al^{3+} cross-links, the polymers form dual-responsive hydrogels in a pH-responsive fashion. Gel degradation and concomitant release of trapped cargo are triggered either by lowering pH and cleaving the cross-links, or by translation of a molecular signal, dithiothreitol, to a macroscopic response by virtue of depolymerization of the self-immolative backbone. As such, the two functionalities represent two orthogonal pathways to hydrogel degradation, working in different time regimes. Both processes result in vanishing gels and release of small molecule cargo. Thus, molecular signals are amplified to a macroscopic response, with the option of leaving only small molecules behind. Controlling material response in different environments is useful for storing and releasing small molecules, which we illustrated by release of rhodamine 6G. This work on highly functionalized, degradable polymers expands the scope of self-immolative polymers, and presents a material capable of releasing small molecules on demand, with the option of concomitant transformation from a polymeric structure into small molecules. Thus, we show that functionalization of self-immolative polymer backbones results in versatile and stimuli-responsive polymeric materials.

Acknowledgements

Funding from the Independent Research Fund Denmark (grant no. 9041-00096B) and Aarhus University is gratefully acknowledged. Affiliation with the Center for Integrated Materials Research (iMAT) at Aarhus University is gratefully acknowledged. Affiliation with the Smart Polymer Materials and Nano-Composites (SPOMAN) Open Science Initiative is gratefully acknowledged.

Conflict of Interest

The authors declare no conflict of interest.

Keywords: catechol · hydrogel · polymers · self-immolative · stimuli-responsive

[1] Q. V. Nguyen, D. P. Huynh, J. H. Park, D. S. Lee, *Eur. Polym. J.* **2015**, *72*, 602 – 619.
[2] Q. Shi, H. Liu, D. D. Tang, Y. H. Li, X. J. Li, F. Xu, *NPG Asia Mater.* **2019**, *11*, 64.
[3] D. Zhang, B. Ren, Y. Zhang, L. Xu, Q. Huang, Y. He, X. Li, J. Wu, J. Yang, Q. Chen, Y. Chang, J. Zheng, *J. Mater. Chem. B* **2020**, *8*, 3171 – 3191; S. Xia, Q. Zhang, S. X. Song, L. J. Duan, G. H. Gao, *Chem. Mater.* **2019**, *31*, 9522 – 9531.
[4] Q. Zhang, C. Y. Shi, D. H. Qu, Y. T. Long, B. L. Feringa, H. Tian, *Sci. Adv.* **2018**, *4*, eaat8192.
[5] A. Andersen, M. Krogsgaard, H. Birkedal, *Biomacromolecules* **2018**, *19*, 1402 – 1409; M. Krogsgaard, M. A. Behrens, J. S. Pedersen, H. Birkedal, *Biomacromolecules* **2013**, *14*, 297 – 301.
[6] M. Krogsgaard, M. R. Hansen, H. Birkedal, *J. Mater. Chem. B* **2014**, *2*, 8292 – 8297.
[7] D. Lu, M. Zhu, S. Wu, Q. Lian, W. Wang, D. Adlam, J. A. Hoyland, B. R. Saunders, *Adv. Funct. Mater.* **2020**, *30*, 1909359.
[8] Y. Chen, W. Wang, D. Wu, H. Zeng, D. G. Hall, R. Narain, *ACS Appl. Mater. Interfaces* **2019**, *11*, 44742 – 44750.
[9] F. Trotta, F. Caldera, C. Dianzani, M. Argenziano, G. Barrera, R. Cavalli, *ChemPlusChem* **2016**, *81*, 439 – 443.
[10] K. Cai, J. Yen, Q. Yin, Y. Liu, Z. Song, S. Lezmi, Y. Zhang, X. Yang, W. G. Helferich, J. Cheng, *Biomater. Sci.* **2015**, *3*, 1061 – 1065.
[11] Y. Zhang, Q. Yin, L. Yin, L. Ma, L. Tang, J. Cheng, *Angew. Chem. Int. Ed.* **2013**, *52*, 6435 – 6439; *Angew. Chem.* **2013**, *125*, 6563 – 6567.
[12] Q. Zhang, Y. X. Deng, C. Y. Shi, B. L. Feringa, H. Tian, D. H. Qu, *Matter* **2021**, *4*, 1352 – 1364.
[13] Y. Xiao, X. Tan, Z. Li, K. Zhang, *J. Mater. Chem. B* **2020**, *8*, 6697 – 6709; Q. E. A. Sirianni, A. Rabiee Kenaree, E. R. Gillies, *Macromolecules* **2019**, *52*, 262 – 270; A. P. Esser-Kahn, N. R. Sottos, S. R. White, J. S. Moore, *J. Am. Chem. Soc.* **2010**, *132*, 10266 – 10268.
[14] S. Gnaim, D. Shabat, *J. Am. Chem. Soc.* **2017**, *139*, 10002 – 10008.
[15] G. G. Lewis, J. S. Robbins, S. T. Phillips, *Chem. Commun.* **2014**, *50*, 5352 – 5354; G. G. Lewis, J. S. Robbins, S. T. Phillips, *Macromolecules* **2013**, *46*, 5177 – 5183.

 © 2021 The Authors. Angewandte Chemie International Edition published by Wiley-VCH GmbH

[16] H. Kim, H. Mohapatra, S. T. Phillips, *Angew. Chem. Int. Ed.* **2015**, *54*, 13063 – 13067; *Angew. Chem.* **2015**, *127*, 13255 – 13259.
[17] M. S. Baker, H. Kim, M. G. Olah, G. G. Lewis, S. T. Phillips, *Green Chem.* **2015**, *17*, 4541 – 4545.
[18] C. Ergene, E. F. Palermo, *J. Mater. Chem. B* **2018**, *6*, 7217 – 7229.
[19] E. M. Lloyd, H. Lopez Hernandez, E. C. Feinberg, M. Yourdkhani, E. K. Zen, E. B. Mejia, N. R. Sottos, J. S. Moore, S. R. White, *Chem. Mater.* **2019**, *31*, 398 – 406.
[20] B. Fan, R. Salazar, E. R. Gillies, *Macromol. Rapid Commun.* **2018**, *39*, 1800173.
[21] S. Pal, A. Sommerfeldt, M. B. Davidsen, M. Hinge, S. U. Pedersen, K. Daasbjerg, *Macromolecules* **2020**, *53*, 4685 – 4691.
[22] A. P. Bapat, B. S. Sumerlin, A. Sutti, *Mater. Horiz.* **2020**, *7*, 694 – 714; R. Guo, Q. Su, J. Zhang, A. Dong, C. Lin, J. Zhang, *Biomacromolecules* **2017**, *18*, 1356 – 1364.
[23] Y. Xu, Y. Li, Q. Chen, L. Fu, L. Tao, Y. Wei, *Int. J. Mol. Sci.* **2018**, *19*, 2198.
[24] Z. Wei, J. H. Yang, X. J. Du, F. Xu, M. Zrinyi, Y. Osada, F. Li, Y. M. Chen, *Macromol. Rapid Commun.* **2013**, *34*, 1464 – 1470.
[25] Q. An, I. D. Wessely, Y. Matt, Z. Hassan, S. Bräse, M. Tsotsalas, *Polym. Chem.* **2019**, *10*, 672 – 678; M. M. Perera, N. Ayres, *Polym. Chem.* **2020**, *11*, 1410 – 1423.
[26] J. C. Lai, L. Li, D. P. Wang, M. H. Zhang, S. R. Mo, X. Wang, K. Y. Zeng, C. H. Li, Q. Jiang, X. Z. You, J. L. Zuo, *Nat. Commun.* **2018**, *9*, 2725; Y. F. Lei, W. Y. Huang, Q. P. Huang, A. Q. Zhang, *New J. Chem.* **2019**, *43*, 261 – 268.
[27] N. Holten-Andersen, M. J. Harrington, H. Birkedal, B. P. Lee, P. B. Messersmith, K. Y. Lee, J. H. Waite, *Proc. Natl. Acad. Sci. USA* **2011**, *108*, 2651 – 2655.
[28] G. Liu, Q. Yuan, G. Hollett, W. Zhao, Y. Kang, J. Wu, *Polym. Chem.* **2018**, *9*, 3436 – 3449.
[29] A. Andersen, Y. Chen, H. Birkedal, *Biomimetics* **2019**, *4*, 30 – 49.
[30] J. Saiz-Poseu, J. Mancebo-Aracil, F. Nador, F. Busque, D. Ruiz-Molina, *Angew. Chem. Int. Ed.* **2019**, *58*, 696 – 714; *Angew. Chem.* **2019**, *131*, 706 – 725; J. Zhou, Z. Lin, Y. Ju, M. A. Rahim, J. J. Richardson, F. Caruso, *Acc. Chem. Res.* **2020**, *53*, 1269 – 1278; J. Yang, M. A. Cohen Stuart, M. Kamperman, *Chem. Soc. Rev.* **2014**, *43*, 8271 – 8298.
[31] Y. Chen, Z. Tan, W. Wang, Y. Y. Peng, R. Narain, *Biomacromolecules* **2019**, *20*, 1028 – 1035; A. R. Narkar, B. Barker, M. Clisch, J. Jiang, B. P. Lee, *Chem. Mater.* **2016**, *28*, 5432 – 5439; Y. J. Kan, E. W. Danner, J. N. Israelachvili, Y. F. Chen, J. H. Waite, *PloS One* **2014**, *9*, e108869.
[32] M. Krogsgaard, V. Nue, H. Birkedal, *Chem. Eur. J.* **2016**, *22*, 844 – 857; M. Krogsgaard, A. Andersen, H. Birkedal, *Chem. Commun.* **2014**, *50*, 13278 – 13281.
[33] H. Lee, N. F. Scherer, P. B. Messersmith, *Proc. Natl. Acad. Sci. USA* **2006**, *103*, 12999 – 13003.
[34] A. H. Agergaard, S. U. Pedersen, H. Birkedal, K. Daasbjerg, *Polym. Chem.* **2020**, *11*, 5572 – 5577.
[35] P. Kord Forooshani, B. P. Lee, *J. Polym. Sci. Part A* **2017**, *55*, 9 – 33; S. Moulay, *Polym. Rev.* **2014**, *54*, 436 – 513.
[36] Y. Li, J. Wen, M. Qin, Y. Cao, H. Ma, W. Wang, *ACS Biomater. Sci. Eng.* **2017**, *3*, 979 – 989; Z. Xu, *Sci. Rep.* **2013**, *3*, 1 – 7.
[37] B. D. B. Tiu, P. Delparastan, M. R. Ney, M. Gerst, P. B. Messersmith, *Angew. Chem. Int. Ed.* **2020**, *59*, 16616 – 16624; *Angew. Chem.* **2020**, *132*, 16759 – 16767.
[38] R. Romero, P. R. Salgado, C. Soto, D. Contreras, V. Melin, *Front. Chem.* **2018**, *6*, 208.
[39] M. S. Menyo, C. J. Hawker, J. H. Waite, *Soft Matter* **2013**, *9*, 10314 – 10323.
[40] V. T. Tran, M. T. I. Mredha, J. Y. Na, J.-K. Seon, J. Cui, I. Jeon, *Chem. Eng. J.* **2020**, *394*, 124941 – 124951.

Manuscript received: June 30, 2021
Accepted manuscript online: July 19, 2021

 © 2021 The Authors. Angewandte Chemie International Edition published by Wiley-VCH GmbH